inorganics

MDPI

Communication

Trimethylammonium Sn(IV) and Pb(IV) Chlorometalate Complexes with Incorporated Dichlorine

Nikita A. Korobeynikov, Andrey N. Usoltsev, Pavel A. Abramov, Vladislav Yu. Komarov, Maxim N. Sokolov and Sergey A. Adonin *

Nikolaev Institute of Inorganic Chemistry SB RAS, 630090 Novosibirsk, Russia
* Correspondence: adonin@niic.nsc.ru

Abstract: Supramolecular dichloro-chlorostannate(IV) and -plumbate(IV) complexes $(Me_3NH)_2\{[MCl_6]Cl_2\}$ (M = Sn (**1**), Pb (**2**)) feature dichlorine units incorporated into a halometalate framework. Both compounds were characterized by X-ray diffractometry and Raman spectroscopy.

Keywords: halide complexes; halogen bonding; tin; lead; Raman spectroscopy

Citation: Korobeynikov, N.A.; Usoltsev, A.N.; Abramov, P.A.; Komarov, V.Y.; Sokolov, M.N.; Adonin, S.A. Trimethylammonium Sn(IV) and Pb(IV) Chlorometalate Complexes with Incorporated Dichlorine. *Inorganics* **2023**, *11*, 25. https://doi.org/10.3390/inorganics11010025

Academic Editors: Axel Klein and Marius Andruh

Received: 11 November 2022
Revised: 19 December 2022
Accepted: 29 December 2022
Published: 3 January 2023

1. Introduction

Anionic halide complexes (halometalates) [1–9] are being intensively investigated for years. Refs. [10–17] In the last decades, this research is strongly promoted by materials science, especially by photovoltaics where iodometalates, especially iodoplumbates(II), are widely used as light absorbers. Refs. [18–24] On the other hand, there are many works focusing on ability of halometalates to build supramolecular associates with di- or polyhalogens due to halogen bonding (XB), and a specific type of non-covalent interactions [25–29]. Although this feature was known for decades, [30–34] its systematic studies began rather recently; Refs. [35,36] in our reports, [37] we demonstrated that such behavior is rather common for Bi(III), Te(IV) and Sb(V) halide complexes. Simultaneously, the works by Shevelkov et al. demonstrated [38–41] that polyiodide-containing iodobismuthates commonly reveal narrow optical band gaps and, sometimes, rather high thermal stability, making such hybrids promising candidates for photovoltaic applications.

For dichlorine-containing halometalates, the very first report was published over 30 years ago. Ref. [42] It was shown that tetramethylammonium chloropalladate(IV) and –stannate(IV) readily form complexes of the general formula $(Me_4N)_2\{[MCl_6](Cl_2)_x\}$, where $X \leq 1$. Surprisingly, this work remained overlooked for years. Only very recently, we demonstrated that such complexes can be formed: a) by other elements, including Te and Pb, and b) in presence of other cations. Refs. [43,44] Continuing this work, we hereby present two new dichlorine-chlorometalates—$(Me_3NH)_2\{[MCl_6]Cl_2\}$ (M = Sn (**1**), Pb (**2**)).

2. Materials and Methods

All reagents were used as purchased. **Caution**: All experiments with Cl_2 require obligatory safety precautions—sufficient exhaust ventilation (fume hood must be used), and obligatory eye (goggles) and skin (gloves) protection. Soluble Pb(II) salts are toxic.

2.1. Preparation of 1

50 mg (0.22 mmol) of $SnCl_2 \cdot 2H_2O$ and 42 mg (0.44 mmol) of Me_3NHCl were dissolved in 4 mL of concentrated HCl at 60 °C. Then gaseous Cl_2 was bubbled through the solution at the same temperature for 10 min. After that, the flask was closed and slowly cooled to room temperature, resulting in the formation of transparent crystals of 1 within several hours. The yield was 69%. The element analysis for $C_6H_{20}N_2SnCl_6$ is (see Discussion): calculated, %: C, 16.00; H, 4.48; N, 6.23; found C, 15.94; H, 4.52; N, 6.29.

2.2. Preparation of 2

111 mg (0.22 mmol) of PbO and 96 mg (1 mmol) of Me_3NHCl were dissolved in 5 mL of concentrated HCl at 60 °C. Then gaseous Cl_2 was bubbled through the solution at the same temperature for 10 min. After that, the flask was closed and slowly cooled to room temperature, resulting in formation of transparent crystals of 1 within several hours. The yield was 71%. The element analysis for $C_6H_{20}N_2PbCl_6$ is (see Discussion): calculated, %: C, 13.38; H, 3.74; N, 5.20; found C, 13.33; H, 3.77; N, 5.27.

2.3. X-Ray Diffractometry

X-ray diffraction data for oligocrystalline samples of $(Me_3NH)_2\{[MCl_6]Cl_2\}$ (M = Sn (**1**), Pb (**2**)) were collected on a Bruker D8 Venture diffractometer (PHOTON III CMOS detector, Mo IμS3.0 X-ray source, Montel mirror focused MoKα radiation λ = 0.71073 Å, N_2-flow cryostat) via 0.5° ω- and φ-scan techniques. The experimental data reductions were performed using the APEX3 suite (Bruker APEX3 Software Suite (APEX3 v.2019.1-0, SADABS v.2016/2, TWINABS v.2012/2, SAINT v.8.40a), Bruker Nonius (2003–2004), Bruker AXS (2005–2018), Bruker Nano (2019): Madison, WI, USA). The only one major crystal domain of **1** and both major domains of **2** were used for the intensity integration via SAINT. Scaling and absorption corrections of the experimental intensities were performed empirically in the medium absorber (3 odd/6 even orders for spherical harmonics, spherical correction μ·r = 0.2) and strong absorber models (7 odd/8 even OSH, μ·r = 1.2) using SADABS and TWINABS programs for **1** and **2**, respectively. The structures were solved by SHELXT [45] and refined using the full-matrix least-squares by SHELXL [46] assisted with Olex2 GUI [47].

Non-H atoms for all structures were located from the electron density map and refined in the anisotropic approximation. H atoms were located from the electron difference maps and refined in a riding model with the constrained U_{iso}. Site occupation factors of Cl atoms of guest Cl_2 molecules, located around special positions (Wyckoff positions 6a, 32 point symmetry) were fixed as 1/3 (i.e., the guest positions are singly occupied by Cl_2 molecules). The crystallographic characteristics, experimental data, and structure refinement indicators are shown in Table 1. The crystallographic data and experimental details were deposited in the Cambridge Crystallographic Data Centre under the deposition codes CCDC 2154812 (**1**) and 2167558 (**2**) and can be obtained at https://www.ccdc.cam.ac.uk/structures (accessed on 10 November 2022).

Table 1. Details of the XRD experiments for **1** and **2**.

	1	**2**
Empirical formula	$C_6H_{20}Cl_8N_2Sn$	$C_6H_{20}Cl_8N_2Pb$
Formula weight	522.53	611.03
Temperature, K	150(2)	250(2)
Crystal system	Trigonal	trigonal
Space group	R–3c	R–3c
a, Å/α, °	9.4097(6)/90	9.5183(2)/90
b, Å/β, °	9.4097(6)/90	9.5183(2)/90
c, Å/γ, °	36.738(3)/120	37.3034(8)/120
Volume, $Å^3$	2817.1(4)	2926.83(14)
Z	6	6
ρ_{calc}, g/cm^3	1.848	2.080
μ, mm^{-1}	2.482	9.726
F(000)	1536.0	1728.0
Crystal size, mm^3	0.13 × 0.08 × 0.05	0.15 × 0.15 × 0.15
Radiation	MoKα (λ = 0.71073)	MoKα (λ = 0.71073)

Table 1. *Cont.*

	1	**2**
2θ range for data collection, °	5.47/62.95	6.55/63.03
Index ranges	$-13 \leq h \leq 13$, $-12 \leq k \leq 13$, $-53 \leq l \leq 53$	$-12 \leq h \leq 0$, $0 \leq k \leq 13$, $0 \leq l \leq 54$ *
Reflections collected/independent	12026/1019	25228 **/1082
R_{int}/R_{σ}	0.0438/0.0196	0.0371/0.0106
Data/restraints/parameters	1019/0/34	1082/0/34
Goodness-of-fit on F^2	1.116	1.112
R_1/wR_2 for $I \geq 2\sigma(I)$	0.0179/0.0388	0.0206/0.0376
for all data	0.0197/0.0394	0.0282/0.0401
Largest diff. peak/hole/e $Å^{-3}$	0.23/–0.36	0.41/–0.47

2.4. Raman Spectroscopy

Raman spectra were collected using a LabRAM HR Evolution (Horiba) spectrometer with the excitation by the 633 nm line of the He-Ne laser. The spectra at room temperatures were obtained in the backscattering geometry with a Raman microscope. The laser beam was focused to a diameter of 2 μm using a LMPlan FL 50×/0.50 Olympus objective. The spectral resolution was 0.7 cm^{-1}. The laser power on the sample surface was about 0.03 mW.

3. Results and Discussion

Both complexes were prepared via bubbling of Cl_2 through HCl solution of corresponding chlorometalate(IV) (in the case of Pb, it is generated in situ during dissolution of oxide in HCl) with trimethylammonium chloride, resulting in crystals suitable for XRD. Both compounds are isostructural. There are mononuclear $[MCl_6]^{2-}$ anions (M-Cl = 2.425–2.427 and 2.504–2.507 Å for Sn and Pb, respectively). Similar to $(Me_4N)_2\{[MCl_6](Cl_2)\}$ (M = Sn, Pb) described earlier [43], the dichlorine units (the Cl-Cl bond lengths are 1.994 in **1** and 1.996 in **2**, respectively) are disordered over three positions with equal occupancies so the system of Cl···Cl non-covalent interactions (Figure 1) is three-dimensional (Cl···Cl = 2.900 and 2.892 Å, M-Cl-Cl = 159.1 and 160.0°, respectively). The proximity of the measured intramolecular Cl-Cl distances to "canonical" values as well as the low anisotropy of the atomic displacements indicates the absence of significant librations of the guest molecules. The crystal packing in **1** and **2** are shown on Figure 2. Details of cation···anion interactions (figures demonstrating minor differences in NH···Cl distances) are given in Supplementary Materials.

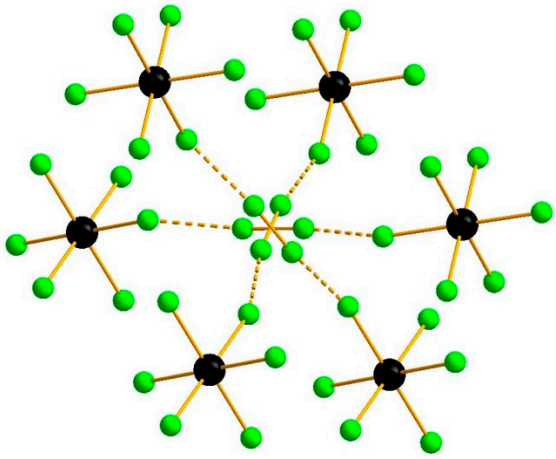

Figure 1. Cl···Cl interactions (dashed) in the structures of **1** and **2**. Metal: black, Cl: light green.

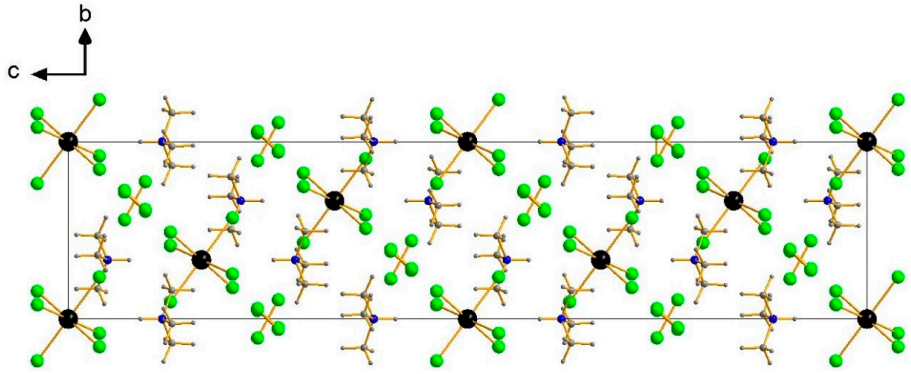

Figure 2. Crystal packing in the structures of **1** and **2**. C and H: grey, N: deep blue, metal: black, Cl: light green.

Both complexes demonstrate poor stability while kept outside the Cl_2-containing mother liquor, and lose Cl_2, transforming into $(Me_3NH)_2[MCl_6]$, as follows from element analysis of residues (see Experimental part). The PXRD data (Figures 3 and 4) confirm that after 1 h the samples of **1** and **2** contain up to 33% of "dichlorine-free" salts (for comparison of the structural data, we used the XRD information for $(Me_3NH)_2[SnCl_6]$ which was described earlier [48]; the $(Me_3NH)_2[PbCl_6]$ salt was found to be isostructural).

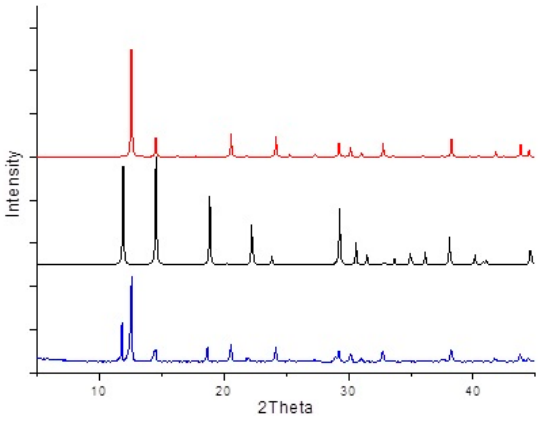

Figure 3. Experimental PXRD pattern of the sample of **1** after 1 h (blue) and calculated patterns of **1** (black) and "dichlorine-free" $(Me_3NH)_2[SnCl_6]$ (red).

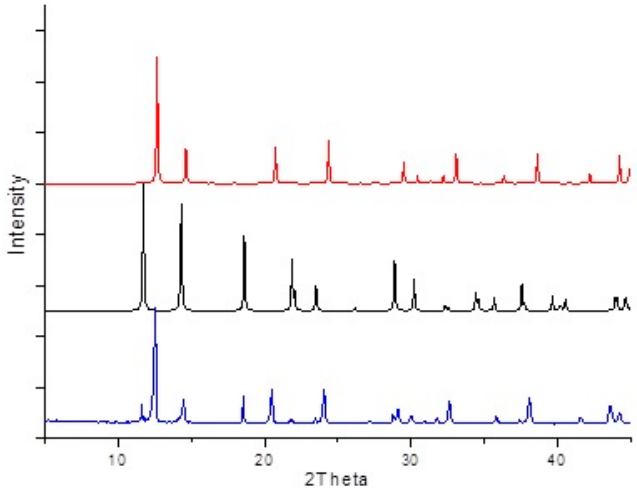

Figure 4. Experimental PXRD pattern of sample **2** after 1 h (blue) and calculated patterns of **2** (black) and "dichlorine-free" $(Me_3NH)_2[PbCl_6]$ (red).

It is worth mentioning that supramolecular complexes with halide···dichlorine non-covalent interactions are yet very rare. Apart from polychlorides extensively studied in last decade by Riedel et al. [49–51], the number of such examples is very limited.

Hirshfeld surface analysis of the structures of **1** and **2** is given in Supplementary Materials. The stability of compounds did not allow performance of TGA experiments; however, we succeeded in recording of Raman spectra (Figures 5 and 6). The bands corresponding to the $\{Cl_2\}$ unit vibrations (518–531 and 508–520 cm^{-1}, respectively) are shifted to the lower wavelengths; this is a common feature for the compound of this family [43] (for gaseous Cl_2, the bands were detected at 539, 547 and 554 cm^{-1} [52]). There are also bands at 312, 242, 165 cm^{-1} for **1** and 278, 218, 143 cm^{-1} for **2** corresponding to ν_1, ν_2 (stretching) and ν_5 (deformation) vibrations in $\{MCl_6\}$ octahedral units [53].

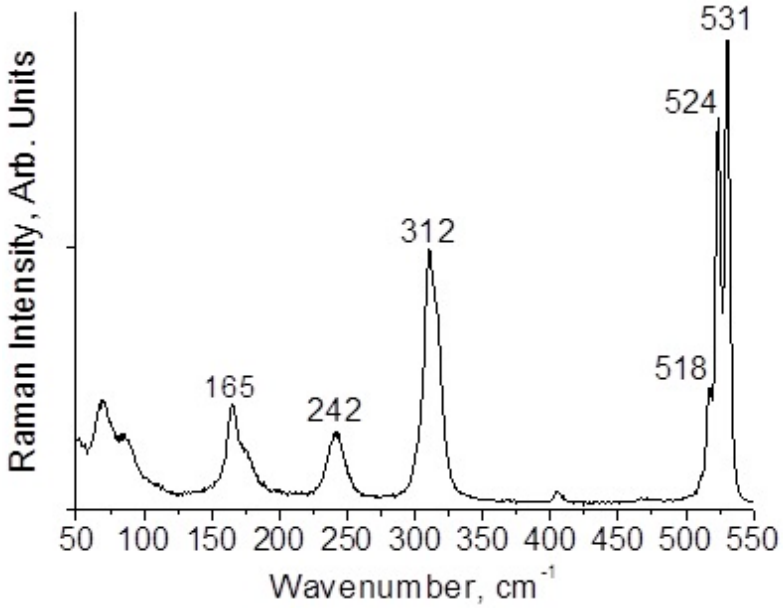

Figure 5. Raman spectrum of **1**.

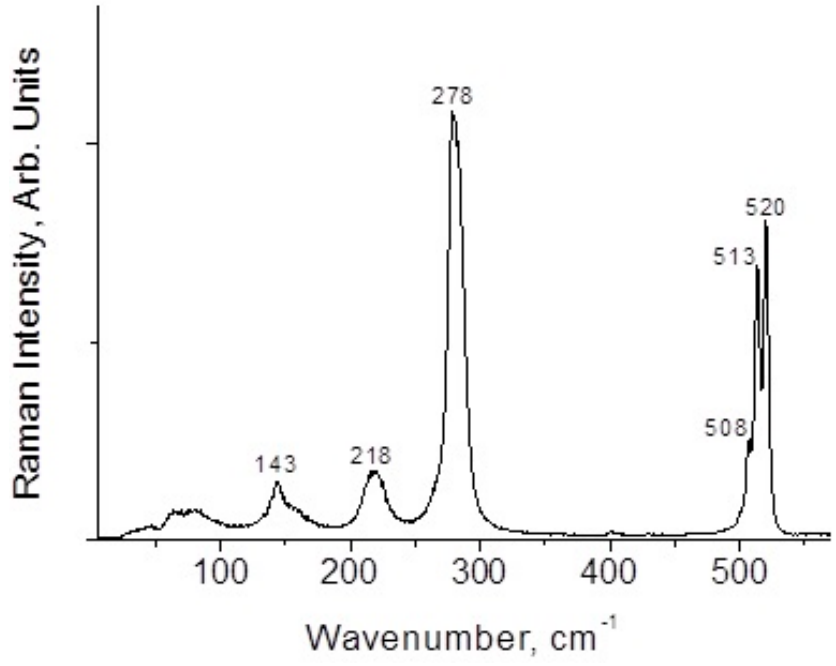

Figure 6. Raman spectrum of **2**.

4. Conclusions

To conclude, the series of Sn and Pb dichlorine-contanining supramolecular compounds featuring Type I Cl···Cl interactions (according to the classification proposed by Metrangolo et al. [54]) was expanded by adding two new complexes. It is noteworthy that, unlike tetramethylammonium-containing relatives, **1** and **2** demonstrate poor stability. This observation confirms the crucial role of multiple cation···anion hydrogen bonds in overall stabilization of the compounds of this type. While all complexes of this family reported contained dichlorine units, we, as stated previously [43], cannot exclude the existence of compounds where other, more sophisticated polychlorine fragments would be stabilized (the overall progress in research of polychlorides [49,50,55] encourages this hypothesis). The corresponding experiments are underway in our group.

Supplementary Materials: The following supporting information can be download at: https://www.mdpi.com/article/10.3390/inorganics11010025/s1, Hirshfeld surface analysis for **1** and **2**.

Author Contributions: Conceptualization, S.A.A. methodology, S.A.A.; validation, A.N.U., P.A.A. and S.A.A.; formal analysis, S.A.A.; investigation, N.A.K., P.A.A. and V.Y.K.; resources, S.A.A.; data curation, P.A.A., V.Y.K. and S.A.A.; writing—original draft preparation, M.N.S. and S.A.A.; writing—review and editing, M.N.S.; visualization, N.A.K., A.N.U., M.N.S. and S.A.A.; supervision, A.N.U. and M.N.S.; project administration, S.A.A.; funding acquisition, S.A.A. All authors have read and agreed to the published version of the manuscript.

Funding: This research was funded by the Russian Science Foundation, grant number 18-73-10040 and, in part, by the Ministry of Science and Higher Education of the Russian Federation (structural characterization of the samples, number 121031700313-8).

Institutional Review Board Statement: Not applicable.

Informed Consent Statement: Not applicable.

Data Availability Statement: See XRD part.

Acknowledgments: The authors thank the XRD facility of NIIC SB RAS and personally thank A. Sukhikh for assistance.

Conflicts of Interest: The authors declare no conflict of interest.

References

1. Szklarz, P.; Śmiałkowski, M.; Bator, G.; Jakubas, R.; Cichos, J.; Karbowiak, M.; Medycki, W.; Baran, J. Phase transitions and properties of 0D hybrid iodoantimonate(III) and iodobismuthate(III) semiconducting ferroics: $[C(NH_2)_3]_3Bi_2I_9$ and $[C(NH_2)_3]_3Sb_2I_9$. *J. Mol. Struct.* **2021**, *1226*, 129387. [CrossRef]
2. Piecha, A.; Jakubas, R.; Pietraszko, A.; Baran, J. Structural characterization and spectroscopic properties of imidazolium chlorobismuthate(III): [C3H5N2]6[Bi4Cl18]. *J. Mol. Struct.* **2007**, *844–845*, 132–139. [CrossRef]
3. Przesławski, J.; Piecha-Bisiorek, A.; Jakubas, R. Specific heat anomaly in ferroelectric: Bis(imidazolium) pentachloroantimonate(III) $(C_3N_2H_5)_2[SbCl_5]$. *J. Mol. Struct.* **2016**, *1110*, 97–101. [CrossRef]
4. Wojtaś, M.; Jakubas, R.; Ciunik, Z.; Medycki, W. Structure and phase transitions in $[(CH_3)4_P]_3[Sb_2Br_9]$ and $[(CH_3)_4P]_3[Bi_2Br_9]$. *J. Solid State Chem.* **2004**, *177*, 1575–1584. [CrossRef]
5. Ouasri, A.; Jeghnou, H.; Rhandour, A.; Roussel, P. Structures and phases transition in hexylenediammonium pentachlorobismuthate (III) $[NH_3(CH_2)_6NH_3]BiCl_5$ crystal. *J. Solid State Chem.* **2013**, *200*, 22–29. [CrossRef]
6. Hrizi, C.; Trigui, A.; Abid, Y.; Chniba-Boudjada, N.; Bordet, P.; Chaabouni, S. α- to β-$[C_6H_4(NH_3)_2]_2Bi_2I_{10}$ reversible solid-state transition, thermochromic and optical studies in the p-phenylenediamine-based iodobismuthate(III) material. *J. Solid State Chem.* **2011**, *184*, 3336–3344. [CrossRef]
7. Ahern, J.C.; Nicholas, A.D.; Kelly, A.W.; Chan, B.; Pike, R.D.; Patterson, H.H. A terbium chlorobismuthate(III) double salt: Synthesis, structure, and photophysical properties. *Inorg. Chim. Acta* **2018**, *478*, 71–76. [CrossRef]
8. Kelly, A.W.; Nicholas, A.; Ahern, J.C.; Chan, B.; Patterson, H.H.; Pike, R.D. Alkali metal bismuth(III) chloride double salts. *J. Alloys Compd.* **2016**, *670*, 337–345. [CrossRef]
9. Moyet, M.A.; Kanan, S.M.; Varney, H.M.; Abu-Farha, N.; Gold, D.B.; Lain, W.J.; Pike, R.D.; Patterson, H.H. Synthesis and characterization of $(RPh_3P)_3$ $[Bi_3I_{12}]$ (R = Me, Ph) iodobismuthate complexes for photocatalytic degradation of organic pollutants. *Res. Chem. Intermed.* **2019**, *45*, 5919–5933. [CrossRef]
10. Wu, L.-M.; Wu, X.-T.; Chen, L. Structural overview and structure–property relationships of iodoplumbate and iodobismuthate. *Coord. Chem. Rev.* **2009**, *253*, 2787–2804. [CrossRef]

11. Buikin, P.A.; Ilyukhin, A.B.; Laurinavichyute, V.K.; Kotov, V.Y. Methylviologen Bromobismuthates. *Russ. J. Inorg. Chem.* **2021**, *66*, 133–138. [CrossRef]
12. Buikin, P.A.; Rudenko, A.Y.; Ilyukhin, A.B.; Kotov, V.Y. Synthesis and Properties of Hybrid Halobismuthates of N-Acetonylpyridinium Derivatives. *Russ. J. Inorg. Chem.* **2021**, *66*, 482–489. [CrossRef]
13. Buikin, P.A.; Rudenko, A.Y.; Ilyukhin, A.B.; Simonenko, N.P.; Yorov, K.E.; Kotov, V.Y. Bromobismuthates of 1,1′-(1,N-Alkanediyl)bis(picolines): Synthesis, Thermal Stability, Crystal Structures, and Optical Properties. *Russ. J. Coord. Chem.* **2020**, *46*, 111–118. [CrossRef]
14. Sharutin, V.V.; Sharutina, O.K.; Senchurin, V.S. Tetraphenylbismuth(V) Derivatives Ph_4BiCl, $[Ph_4BiDMSO\text{-}O][PtBr_3DMSO\text{-}S]$ and $[Ph_4Bi]_2[PtCl_6]$: Synthesis and Structure. *Russ. J. Inorg. Chem.* **2020**, *65*, 1712–1717. [CrossRef]
15. Zykova, A.R.; Sharutin, V.V.; Sharutina, O.K.; Senchurin, V.S. Synthesis and Structure of Organyltriphenylphosphonium and Stibonium Hexabromoplatinates. *Russ. J. Gen. Chem.* **2020**, *90*, 1483–1488. [CrossRef]
16. Sharutin, V.V.; Sharutina, O.K.; Lobanova, E.V. Hafnium Complexes $[Ph_3PR]_2$ $[HfCl_6]$, where R = Et, $CH_2C_6H_4CN^{-4}$, or $CH_2C_6H_4F^{-4}$: Synthesis and Structure. *Russ. J. Inorg. Chem.* **2020**, *65*, 870–873. [CrossRef]
17. Yelovik, N.A.; Shestimerova, T.A.; Bykov, M.A.; Wei, Z.; Dikarev, E.V.; Shevelkov, A.V. Synthesis, structure, and properties of $LnBiI_6 \bullet 13H_2O$ (Ln = La, Nd). *Russ. Chem. Bull.* **2017**, *66*, 1196–1201. [CrossRef]
18. Udalova, N.N.; Tutantsev, A.S.; Fateev, S.A.; Zharenova, E.A.; Belich, N.A.; Nemygina, E.M.; Ryabova, A.V.; Goodilin, E.A.; Tarasov, A.B. Crystallization Features of $MAPbI_3$ Hybrid Perovskite during the Reaction of PbI_2 with Reactive Polyiodide Melts. *Russ. J. Inorg. Chem.* **2021**, *66*, 153–162. [CrossRef]
19. Belich, N.A.; Tychinina, A.S.; Kuznetsov, V.V.; Goodilin, E.A.; Grätzel, M.; Tarasov, A.B. Template synthesis of methylammonium lead iodide in the matrix of anodic titanium dioxide via the direct conversion of electrodeposited elemental lead. *Mendeleev Commun.* **2018**, *28*, 487–489. [CrossRef]
20. Fateev, S.A.; Petrov, A.A.; Khrustalev, V.N.; Dorovatovskii, P.V.; Zubavichus, Y.V.; Goodilin, E.A.; Tarasov, A.B. Solution Processing of Methylammonium Lead Iodide Perovskite from γ-Butyrolactone: Crystallization Mediated by Solvation Equilibrium. *Chem. Mater.* **2018**, *30*, 5237–5244. [CrossRef]
21. Petrov, A.A.; Sokolova, I.P.; Belich, N.A.; Peters, G.S.; Dorovatovskii, P.V.; Zubavichus, Y.V.; Khrustalev, V.N.; Petrov, A.V.; Grätzel, M.; Goodilin, E.A.; et al. Crystal Structure of DMF-Intermediate Phases Uncovers the Link between $CH_3NH_3PbI_3$ Morphology and Precursor Stoichiometry. *J. Phys. Chem. C* **2017**, *121*, 20739–20743. [CrossRef]
22. Frolova, L.A.; Anokhin, D.V.; Piryazev, A.A.; Luchkin, S.Y.; Dremova, N.N.; Stevenson, K.J.; Troshin, P.A. Highly Efficient All-Inorganic Planar Heterojunction Perovskite Solar Cells Produced by Thermal Coevaporation of CsI and PbI_2. *J. Phys. Chem. Lett.* **2017**, *8*, 67–72. [CrossRef]
23. Fateev, S.A.; Petrov, A.A.; Marchenko, E.I.; Zubavichus, Y.V.; Khrustalev, V.N.; Petrov, A.V.; Aksenov, S.M.; Goodilin, E.A.; Tarasov, A.B. FA_2PbBr_4: Synthesis, Structure, and Unusual Optical Properties of Two Polymorphs of Formamidinium-Based Layered (110) Hybrid Perovskite. *Chem. Mater.* **2021**, *33*, 1900–1907. [CrossRef]
24. Tutantsev, A.S.; Udalova, N.N.; Fateev, S.A.; Petrov, A.A.; Petrov, A.A.; Chengyuan, W.; Maksimov, E.G.; Goodilin, E.A.; Goodilin, E.A.; Tarasov, A.B.; et al. New Pigeonholing Approach for Selection of Solvents Relevant to Lead Halide Perovskite Processing. *J. Phys. Chem. C* **2020**, *124*, 11117–11123. [CrossRef]
25. Desiraju, G.R.; Ho, P.S.; Kloo, L.; Legon, A.C.; Marquardt, R.; Metrangolo, P.; Politzer, P.; Resnati, G.; Rissanen, K. Definition of the halogen bond (IUPAC Recommendations 2013). *Pure Appl. Chem.* **2013**, *85*, 1711–1713. [CrossRef]
26. Aliyarova, I.S.; Ivanov, D.M.; Soldatova, N.S.; Novikov, A.S.; Postnikov, P.S.; Yusubov, M.S.; Kukushkin, V.Y. Bifurcated Halogen Bonding Involving Diaryliodonium Cations as Iodine(III)-Based Double-σ-Hole Donors. *Cryst. Growth Des.* **2021**, *21*, 1136–1147. [CrossRef]
27. Mikherdov, A.S.; Novikov, A.S.; Boyarskiy, V.P.; Kukushkin, V.Y. The halogen bond with isocyano carbon reduces isocyanide odor. *Nat. Commun.* **2020**, *11*, 2921. [CrossRef]
28. Soldatova, N.S.; Postnikov, P.S.; Suslonov, V.V.; Kissler, T.Y.; Ivanov, D.M.; Yusubov, M.S.; Galmés, B.; Frontera, A.; Kukushkin, V.Y. Diaryliodonium as a double s-hole donor: The dichotomy of thiocyanate halogen bonding provides divergent solid state arylation by diaryliodonium cations. *Org. Chem. Front.* **2020**, *7*, 2230–2242. [CrossRef]
29. Bokach, N.A.; Suslonov, V.V.; Eliseeva, A.A.; Novikov, A.S.; Ivanov, D.M.; Dubovtsev, A.Y.; Kukushkin, V.Y.; Kukushkin, V.Y. Tetrachloroplatinate(ii) anion as a square-planar tecton for crystal engineering involving halogen bonding. *CrystEngComm* **2020**, *22*, 4180–4189.
30. Lawton, S.L.; McAfee, E.R.; Benson, J.E.; Jacobson, R.A. Crystal structure of quinolinium hexabromoantimonate(V) tribromide, $(C_9H_7NH)_2Sb^{V}Br_9$. *Inorg. Chem.* **1973**, *12*, 2939–2944. [CrossRef]
31. Hubbard, C.R.; Jacobson, R.A. Molecular bromine bridging of $Sb^{III}{}_2Br_9{}^{3-}$ anions and the crystal structure of tetraethylammonium nonabromodiantimonate(III)-dibromine. *Inorg. Chem.* **1972**, *11*, 2247–2250. [CrossRef]
32. Lawton, S.L.; Jacobson, R.A. Crystal structure of di-.alpha.-picolinium nonabromoantimonate(V). *Inorg. Chem.* **1968**, *7*, 2124–2134. [CrossRef]
33. Siepmann, R.; von Schnering, H.G. Die Kristallstruktur von W6Br16. Eine Verbindung mit Polykationen [W6Br8]6+ und Polyanionen [Br4]2−. *Z. Anorg. Allg. Chem.* **1968**, *357*, 289–298. [CrossRef]
34. Berkei, M.; Bickley, J.F.; Heaton, B.T.; Steiner, A. Polymeric anionic networks using dibromine as a crosslinker; the preparation and crystal structure of $[(C_4H_9)_4N]_2[Pt_2Br_{10}]\cdot(Br_2)_7$ and $[(C_4H_9)_4N]_2[PtBr_4Cl_2]\cdot(Br_2)_6$. *Chem. Commun.* **2002**, 2180–2181. [CrossRef]

35. Hausmann, D.; Feldmann, C. Bromine-rich Zinc Bromides: Zn_6Br_{12}(18-crown-6)$_2\times(Br_2)_5$, Zn_4Br_8(18-crown-6)$_2\times(Br_2)_3$, and Zn_6Br_{12}(18-crown-6)$_2\times(Br_2)_2$. *Inorg. Chem.* **2016**, *55*, 6141–6147. [CrossRef]
36. Eich, A.; Köppe, R.; Roesky, P.W.; Feldmann, C. The Bromine-Rich Bromido Metallates $[BMIm]_2[SnBr_6]\cdot(Br_2)$ and [MnBr(18-crown-6)]$_4[SnBr_6]_2\cdot(Br_2)_{4.5}$. *Eur. J. Inorg. Chem.* **2019**, *2019*, 1292–1298. [CrossRef]
37. Adonin, S.A.; Gorokh, I.D.; Novikov, A.S.; Samsonenko, D.G.; Plyusnin, P.E.; Sokolov, M.N.; Fedin, V.P. Bromine-rich complexes of bismuth: Experimental and theoretical studies. *Dalt. Trans.* **2018**, *47*, 2683–2689. [CrossRef]
38. Shestimerova, T.A.; Golubev, N.A.; Bykov, M.A.; Mironov, A.V.; Fateev, S.A.; Tarasov, A.B.; Turkevych, I.; Wei, Z.; Dikarev, E.V.; Shevelkov, A.V. Molecular and supramolecular structures of triiodides and polyiodobismuthates of phenylenediammonium and its n,n-dimethyl derivative. *Molecules* **2021**, *26*, 5712. [CrossRef]
39. Shestimerova, T.A.; Yelavik, N.A.; Mironov, A.V.; Kuznetsov, A.N.; Bykov, M.A.; Grigorieva, A.V.; Utochnikova, V.V.; Lepnev, L.S.; Shevelkov, A.V. From isolated anions to polymer structures through linking with I_2: Synthesis, structure, and properties of two complex bismuth(III) iodine iodides. *Inorg. Chem.* **2018**, *57*, 4077–4087. [CrossRef]
40. Shestimerova, T.A.; Mironov, A.V.; Bykov, M.A.; Grigorieva, A.V.; Wei, Z.; Dikarev, E.V.; Shevelkov, A.V. Assembling polyiodides and iodobismuthates using a template effect of a cyclic diammonium cation and formation of a low-gap hybrid iodobismuthate with high thermal stability. *Molecules* **2020**, *25*, 2765. [CrossRef]
41. Shestimerova, T.A.; Golubev, N.A.; Yelavik, N.A.; Bykov, M.A.; Grigorieva, A.V.; Wei, Z.; Dikarev, E.V.; Shevelkov, A.V. Role of I_2 Molecules and Weak Interactions in Supramolecular Assembling of Pseudo-Three-Dimensional Hybrid Bismuth Polyiodides: Synthesis, Structure, and Optical Properties of Phenylenediammonium Polyiodobismuthate(III). *Cryst. Growth Des.* **2018**, *18*, 2572–2578. [CrossRef]
42. Storck, P.; Weiss, A. 35C1NQR and X-Ray Studies of Hexachloropalladates A2PdCl6 (A = Rb, Cs, NH4) and the Cl2—Clathrates Bis(tetramethylammonium)hexachloropalladate (Me4N)2PdCl6 • Cl2 and Bis(tetramethylammonium)hexachlorostannate (Me4N)2SnCl6 • Cl2. *Zeitschrift fur Naturforsch.—Sect. B J. Chem. Sci.* **1991**, *46*, 1214–1218. [CrossRef]
43. Usoltsev, A.N.; Korobeynikov, N.A.; Kolesov, B.A.; Novikov, A.S.; Samsonenko, D.G.; Fedin, V.P.; Sokolov, M.N.; Adonin, S.A. Rule, Not Exclusion: Formation of Dichlorine-Containing Supramolecular Complexes with Chlorometalates(IV). *Inorg. Chem.* **2021**, *60*, 4171–4177. [CrossRef]
44. Usoltsev, A.N.; Adonin, S.A.; Kolesov, B.A.; Novikov, A.S.; Fedin, V.P.; Sokolov, M.N. Opening the Third Century of Polyhalide Chemistry: Thermally Stable Complex with "Trapped" Dichlorine. *Chem.—A Eur. J.* **2020**, *26*, 13776–13778. [CrossRef]
45. Sheldrick, G.M. SHELXT—Integrated space-group and crystal-structure determination. *Acta Crystallogr. Sect. A Found. Adv.* **2015**, *71*, 3–8. [CrossRef]
46. Sheldrick, G.M. Crystal structure refinement with SHELXL. *Acta Crystallogr. Sect. C Struct. Chem.* **2015**, *71*, 3–8. [CrossRef]
47. Dolomanov, O.V.; Bourhis, L.J.; Gildea, R.J.; Howard, J.A.K.; Puschmann, H. OLEX2: A complete structure solution, refinement and analysis program. *J. Appl. Crystallogr.* **2009**, *42*, 339–341. [CrossRef]
48. Knop, O.; Cameron, T.S.; James, M.A.; Falk, M. Alkylammonium hexachlorostannates(IV), $(R_nNH_{4-n})_2SnCl_6$: Crystal structure, infrared spectrum, and hydrogen bonding. *Can. J. Chem.* **1983**, *61*, 1620–1646. [CrossRef]
49. Brückner, R.; Haller, H.; Ellwanger, M.; Riedel, S. Polychloride monoanions from [Cl3]− to [Cl9]−: A Raman spectroscopic and quantum chemical investigation. *Chem.—A Eur. J.* **2012**, *18*, 5741–5747. [CrossRef]
50. Sonnenberg, K.; Pröhm, P.; Schwarze, N.; Müller, C.; Beckers, H.; Riedel, S. Investigation of Large Polychloride Anions: $[Cl_{11}]^-$, $[Cl_{12}]^{2-}$, and $[Cl^{13}]^-$. *Angew. Chem. Int. Ed.* **2018**, *57*, 9136–9140. [CrossRef]
51. Brückner, R.; Pröhm, P.; Wiesner, A.; Steinhauer, S.; Müller, C.; Riedel, S. Structural Proof for the First Dianion of a Polychloride: Investigation of $[Cl_8]^{2-}$. *Angew. Chem. Int. Ed.* **2016**, *55*, 10904–10908. [CrossRef] [PubMed]
52. Aggarwal, R.L.; Farrar, L.W.; Di Cecca, S.; Jeys, T.H. Raman spectra and cross sections of ammonia, chlorine, hydrogen sulfide, phosgene, and sulfur dioxide toxic gases in the fingerprint region 400–1400 cm^{-1}. *AIP Adv.* **2016**, *6*, 025310. [CrossRef]
53. Creighton, J.A.; Woodward, L.A. Raman spectrum of the hexachloroplumbate ion $PbCl_6^{2-}$ in solution. *Trans. Faraday Soc.* **1962**, *58*, 1077–1079. [CrossRef]
54. Cavallo, G.; Metrangolo, P.; Milani, R.; Pilati, R.; Priimagi, A.; Resnati, G.; Terraneo, G. The halogen bond. *Chem. Rev.* **2016**, *116*, 2478–2601. [CrossRef] [PubMed]
55. Voßnacker, P.; Keilhack, T.; Schwarze, N.; Sonnenberg, K.; Seppelt, K.; Malischewski, M.; Riedel, S. From Missing Links to New Records: A Series of Novel Polychlorine Anions. *Eur. J. Inorg. Chem.* **2021**, *2021*, 1034–1040. [CrossRef]